IEEE/CSC & ESAS SUPERCONDUCTIVITY NEWS FORUM (global edition), January 2017 (Preview 2).
This ASC 2016 manuscript 3LPo2D-04 was submitted to *IEEE Trans. Appl. Supercond.* for possible publication.
DOI: 10.1109/TASC.2017.2655108

Design and Manufacturing of a Multistage Cooled Current Lead for Superconducting High Current DC Busbars in Industrial Applications

Florian Schreiner, Bernd Gutheil, Mathias Noe, Wolfgang Reiser, Stefan Huwer, Claus Hanebeck, Carsten Räch, Marcus Röhrenbeck, and Fabian Schreiner

***Abstract*—There is a high potential to use high-temperature superconductors instead of conventional busbars in high direct current industrial applications. Since current leads are typically the major source of losses in these applications, we introduce and investigate the concept of a multistage cooled current lead for an operating current of 20 kA to minimize current lead losses. The design is based on the idea to realize an efficient and at the same time economic current lead that consists of components which are market proven and reliable. The current lead is down to 77 K and is cooled with two intermediate cooling stages at 240 K and 150 K. One key component is the joint between the resistive copper part and the YBCO high-temperature superconductor tapes, which is manufactured by a new soldering process. Moreover, electromagnetic Finite Element Analyses of a high-temperature superconductor stack design have been done to optimize the current carrying capacity of the current lead. As a result, the multistage cooled current lead is designed to cryogenic losses of 22.4 W/kA at 77 K.**

***Index Terms*—Cryogenics, current leads, high-temperature superconductors, low heat leakage, multistage current lead.**

I. Introduction

INDUSTRIAL applications with very high dc currents – like chlorine, zinc or copper electrolysis and aluminum plants – offer a high potential to use high-temperature superconductor (HTS) busbars. In particular aluminum electrolysis plants with currents of more than 200 kA up to 500 kA are highly suitable applications for superconducting busbars [1]. In [2], two different possible configurations are investigated; namely the use of HTS to realize a superconducting power supply line, and also the approach to build a superconducting magnetic field compensating line to achieve a symmetric and well-controlled magnetic field in the electrolysis cells.

This work was supported by the Federal Ministry for Economic Affairs and Energy under Grant KF2367206RR3.

Florian Schreiner, Bernd Gutheil, Marcus Röhrenbeck, and Fabian Schreiner are with the University of Kaiserslautern, 67663 Kaiserslautern, Germany (E-Mail: schreiner@eit.uni-kl.de).

Mathias Noe is with the Institute of Technical Physics at Karlsruhe Institute of Technology, 76344 Eggenstein-Leopoldshafen, Germany (E-Mail: mathias.noe@kit.edu).

Carsten Räch is with the University of Applied Sciences Kaiserslautern, 67657 Kaiserslautern, Germany (E-Mail: carsten.raech@hs-kl.de).

Wolfgang Reiser, Stefan Huwer, and Claus Hanebeck are with the company Vision Electric Super Conductors Ltd., 67663 Kaiserslautern, Germany (E-Mail: reiser@vesc-superbar.de).

In China, an HTS dc power cable with a length of 360 m and a current carrying capacity of 10 kA has already been installed in an aluminum electrolysis plant to serve as a power supply line for the electrolysis process [3], [4]. In this application, Bi-2223 HTS tapes were used to manufacture the cable.

Most industrial high current dc applications have in common, that the lengths of the superconducting busbars are rather short. Therefore, the current leads are typically the major source of losses. Reducing the heat leakage caused by the leads would improve the performance and economy of the whole superconducting busbar system.

II. Design of a Three Stage Cooled Current Lead

A. 1D-Model

A current lead represents the link between conventional room temperature applications and the superconducting systems; it is the component which transfers the electric current from room temperature level to the operating temperature of the superconductors. Optimizing a current lead, the ratio of the length and the cross-section of the lead need to be adapted [5], [6]. Using HTS superconductors in the busbar system at the temperature level of liquid nitrogen, no binary current leads can be applied. Binary current leads consist of a resistive part and a second part made of HTS superconductors to transfer the electric current down to the temperature level of liquid helium [7]–[9]. In this case, pure resistive current leads are considered, because the superconducting busbar system is designed to operate at a temperature level of about 65-77 K.

Initially, we built a 1D-model based on the Finite Difference Method (FDM) to examine and compare three different design approaches of resistive current leads. Fig. 1 shows the temperature profile over the length of a conduction cooled, nitrogen gas cooled, and multistage cooled lead design. Moreover, the respective heat leakages to the 77 K temperature level are pictured. The multistage cooled current lead concept has got two intermediate cooling stages at 240 K, and 150 K. The temperature levels are chosen for economic reasons, since market proven and reliable refrigeration units are available for these temperatures. Table I compares the different heat leakages to the cryogenic temperature level and the overall ideal electric power consumptions of the refrigerators.

We decided to pursue the concept of a multistage cooled lead to be able to decrease the heat leakage to the cryogenic temperature level and furthermore minimize the electric power

IEEE/CSC & ESAS SUPERCONDUCTIVITY NEWS FORUM (global edition), January 2017 (Preview 2).
This ASC 2016 manuscript 3LPo2D-04 was submitted to *IEEE Trans. Appl. Supercond.* for possible publication.
DOI: 10.1109/TASC.2017.2655108

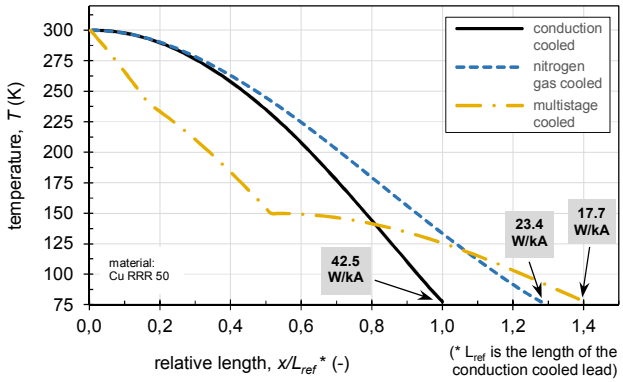

Fig. 1. Temperature profiles of different types of current leads derived from a 1D-model analysis. The figure compares conduction cooled, nitrogen gas cooled, and three stage cooled current lead designs. The respective heat leakages to the cryogenic temperature level at 77 K are also depicted.

TABLE I
COMPARISON OF HEAT LEAKAGE TO THE CRYOGENIC TEMPERATURE LEVEL AND ELECTRIC POWER CONSUMPTION

Current lead design	Heat leakage	Electric power consumption
Conduction Cooled	at 77 K: 42.5 W/kA [10], [11]	123.1 W/kA [a]
Nitrogen gas cooled	at 77 K: 23.4 W/kA [7], [10]	90.6 W/kA [b]
Multistage cooled	at 240 K: 23.2 W/kA at 150 K: 35.6 W/kA at 77 K: 17.7 W/kA	∑: 92.7 W/kA [a]

[a] Calculated with the coefficient of performance of the ideal Carnot cycle (COP_{Carnot})
[b] Calculated with the ideal liquefaction work of nitrogen

consumption.
A multistage cooled current lead has already been investigated in [10]–[14], but, as far as we are aware, has never been realized for an operating current of 20 kA. In [13], a test of a subscale model for a current up to only 5 kA is described.

III. Manufacturing of a Three Stage Cooled Current Lead

A. General Overview

The geometry of our multistage cooled current lead is designed and optimized for an operating current of 20 kA. The resistive current path of the lead is manufactured out of copper and the lead transfers the electric current to an HTS stack.

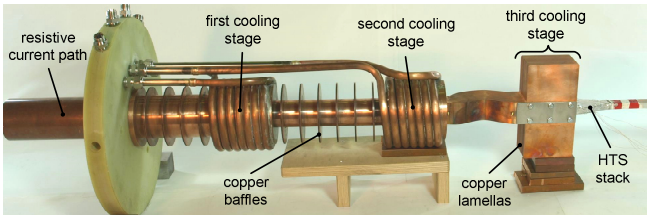

Fig. 2. Current path of the three stage cooled current lead, without cryostat and refrigerator units. Both heat exchangers of the intermediate cooling stages are shown and in addition the transition from copper to the HTS tapes is depicted.

Fig. 2 illustrates the complete current path, including the HTS stack consisting of 96 YBCO tapes. The intermediate cooling stages are designed to operate at a temperature of 240 K and 150 K. The last cooling stage defines the operating temperature of the superconductors and is realized using a liquid nitrogen bath at a temperature of about 77 K. Evaporating liquid nitrogen is condensed by a Cryomech AL-600 cold head. The cooling power at the 240 K cooling stage is provided by a common compression refrigeration machine and the 150 K cooling stage is supplied by a mixed refrigerant Joule-Thomson cooler.

The transition from the resistive copper path to the HTS tapes is done by a novel copper lamella HTS tape connection. This component meets several requirements at once:

- Mechanical compensation element to handle the thermal contractions in the system;
- Uniform current distribution to the HTS tapes because of the nearly equal copper series resistors;
- Large cooling surface to excess the heat load to the liquid nitrogen;
- Good electrical connection between the resistive copper path and the HTS tapes.

B. Soldering Copper Lamellas and HTS Tapes with a Pressure Welding Process

We developed a new soldering process to connect the copper lamellas with the HTS tapes. A pressure welding process has been adapted to join the lamella and the tape very fast, reproducible, and reliable. The copper lamella is 0.5 mm thick, the HTS tape has a thickness of 0.15 mm and a width of 12 mm. A 0.1 mm thin Sn63Pb37 solder tape is placed between the two layers and afterwards this compound is soldered with a pressure welding process. Two graphite electrodes apply pressure, simultaneously a very short current pulse heats up the compound and the solder starts to melt, connecting the copper lamella with the HTS tape. Fig. 3 (a) illustrates such a soldered joint of a copper lamella and an HTS tape.

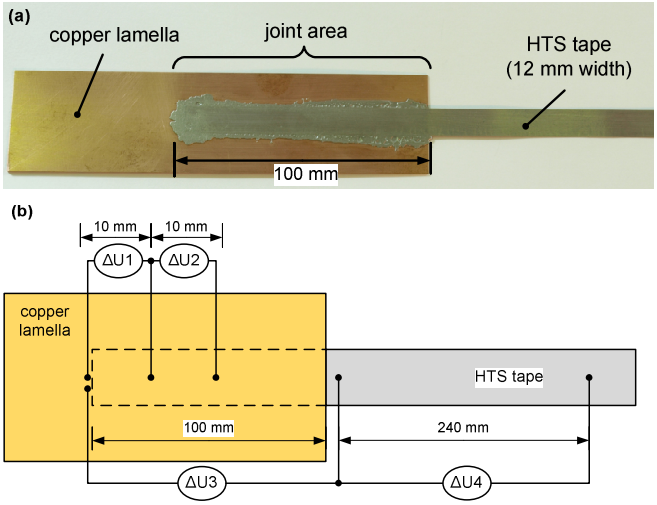

Fig. 3. (a) Soldered joint of a copper lamella and an HTS tape. (b) Technical illustration of the positions of the voltage taps to measure voltage drops along the joint.

IEEE/CSC & ESAS SUPERCONDUCTIVITY NEWS FORUM (global edition), January 2017 (Preview 2).
This ASC 2016 manuscript 3LPo2D-04 was submitted to *IEEE Trans. Appl. Supercond.* for possible publication.
DOI: 10.1109/TASC.2017.2655108

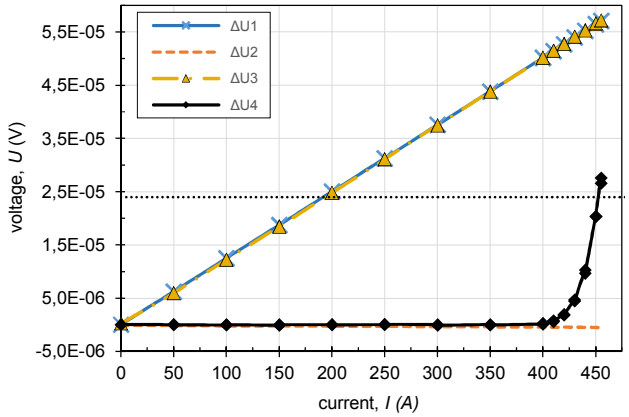

Fig. 4. Voltage drop measurements along the soldered joint between copper lamella and HTS tape. The quench criteria for the superconductor is 24 µV (dotted black line).

C. *Current Coupling Behavior of the Joint*

To examine the current coupling behavior of said joint, we measured voltage drops along the connection. Fig. 3 (b) shows a technical illustration of the positions of the voltage taps. They were attached to the backside of the copper lamella, namely to the side of the lamella which is opposite to the joint. Hence, we measured voltage drops in the resistive copper (*ΔU1*, *ΔU2*). Furthermore, the voltage drop *ΔU3* represents the voltage drop of the entire joint. Additionally, we measured the voltage drop of the HTS tape (*ΔU4*) to be able to identify a quench on the tape. The quench criteria used was about 1 µV/cm. The investigation has been performed in a liquid nitrogen bath at atmospheric pressure.

Fig. 4 depicts the results of the measurement; it shows that the electric current couples immediately into the HTS tape since *ΔU1* is almost equal to *ΔU3* and the voltage drop *ΔU2* is zero. Considering the current coupling behavior, a very short joint length would be sufficient. But a longer joint length also provides thermal and mechanical stability. The HTS tape itself starts to quench at a current of about 450 A (see *ΔU4*).
The total voltage drop of the joint at a current of 450 A is about 56 µV. Accordingly, the generated ohmic loss is approximately 25 mW. In comparison, the pure copper lamella along a length of 100 mm would have a resistance of about 11 µΩ, which correlates to a generated ohmic loss of 2.2 W at a current of 450 A.

IV. Finite Element Analysis of a Three Stage Cooled Current Lead

A. *Coupled Thermal-Electric Analysis*

A coupled thermal-electric 3D Finite Element Analysis (FEA) has been done with the program ANSYS 17.1. The three-dimensional geometry of the resistive current path, including the heat exchanger surfaces, has been modeled. Fixed temperatures of 300 K and 77 K at the warm and cold end, and 240 K and 150 K at the intermediate cooling stages have been used as boundary conditions for the simulation.
Fig. 5 (a) shows the 3D temperature distribution of the current lead. The corresponding temperature profile in longitudinal direction of the current lead is illustrated in Fig. 5 (b). In

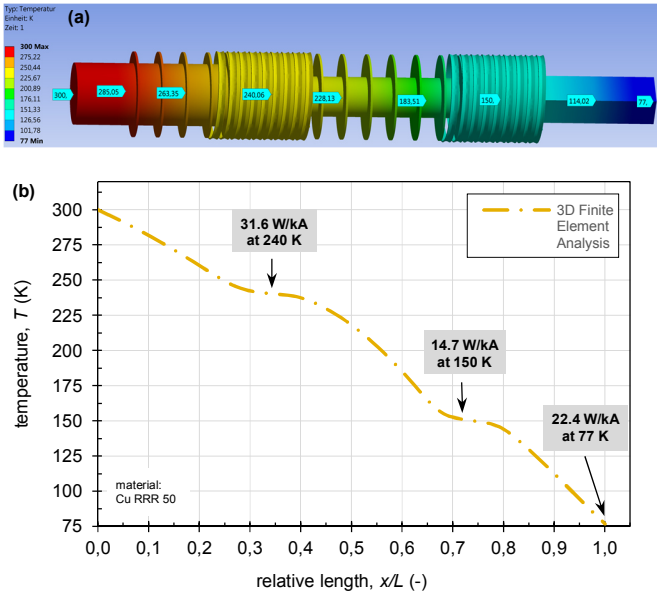

Fig. 5. (a) 3D Finite Element Analysis of the manufactured geometry of the current lead. (b) Temperature profile of the three stage cooled current lead (longitudinal axis). Furthermore, the heat leakages to the three cooling stages are depicted.

TABLE II
Heat Leakages of the Refrigerators and Electric Power Consumption of a Three Stage Cooled Current Lead

Cooling Stage	Heat leakage	Electric power consumption
240 K	31.6 W/kA	7.9 W/kA [a]
150 K	14.7 W/kA	14.7 W/kA [a]
77 K	22.4 W/kA	64.9 W/kA [a]
		∑: 87.5 W/kA

[a] Calculated with the coefficient of performance of the ideal Carnot cycle (COP_{Carnot})

comparison to Fig. 1, the spatial dimensions of the heat exchangers of the intermediate cooling stages are also considered and visible in the temperature profile. The zero-gradient of the temperature profile after the 150 K cooling stage has vanished. We followed the approach to minimize the total electric power consumption of the current lead instead of just minimizing the heat leakage to the cryogenic temperature level [15]. Table II lists the heat leakages of the three cooling stages and the total electric power consumption.

B. *Electromagnetic Analysis of an HTS Stack*

An electromagnetic analysis has been done to design and optimize a stack of HTS tapes to carry 20 kA. The simulation program combines Matlab code and the open source software FEMM 4.2 to simulate the electromagnetic behavior of the superconductors. It is based on the approach described in [16], [17]. The HTS stack consists of 96 tapes, with a tape thickness of 0.15 mm and a distance between two tapes of 0.1 mm. In total, the stack has a height of about 24 mm and a width of 12 mm. The tapes used differ in their current carrying capacities.

IEEE/CSC & ESAS SUPERCONDUCTIVITY NEWS FORUM (global edition), January 2017 (Preview 2).
This ASC 2016 manuscript 3LPo2D-04 was submitted to *IEEE Trans. Appl. Supercond.* for possible publication.
DOI: 10.1109/TASC.2017.2655108

Hence, we divide them in two groups:

- *70* HTS tapes with a predicted critical current of *550 A* (at 77 K and in self-field);
- *26* HTS tapes with a predicted critical current of *400 A* (at 77 K and in self-field).

The 70 HTS tapes with higher critical current are put on the outside of the stack and the 26 HTS tapes with less critical current on the inside, since there is a higher magnetic field penetration on the outside of the stack.

Fig. 6 illustrates the results of two different simulations. In the first case, a uniform current distribution to all 96 HTS tapes is assumed. Every tape of the stack carries the same current. This behavior is determined by the copper lamellas. They act as nearly equal series resistors. The outer tapes of the stack reach their critical currents first. The white diamonds in the diagram indicate the actual possible critical current of each tape in this magnetic field constellation, assuming a uniform current distribution. In the second case, an equipotential configuration of the HTS stack is supposed. Depending on the magnetic field and the resulting critical currents, the total current can distribute to the different tapes in the stack. Both cases result in slightly different total current carrying capabilities of the whole stack:

- Uniform distribution: **22.6 kA**;
- Equipotential stack configuration: **23.9 kA**.

Fig. 7 depicts a 2D plot of the magnetic field in case of a uniform current distribution to the tapes. The field reaches its highest values of about 0.42 T in the outer corners of the stack. It is apparent, that the magnetic field is not completely symmetric.

This effect is caused by the phenomena illustrated in Fig. 8. Standard HTS tapes, without advanced pinning, show a behavior of the critical current in dependency on the angle of the magnet field vector indicated by the black line in the diagram. Usually, the critical current of such tapes reaches its minimum, if magnetic field penetrates perpendicularly to the tape. In comparison, the tapes used in our current lead have a shift of about 30° in the data. This shift is caused by the manufacturing process of these tapes [18].

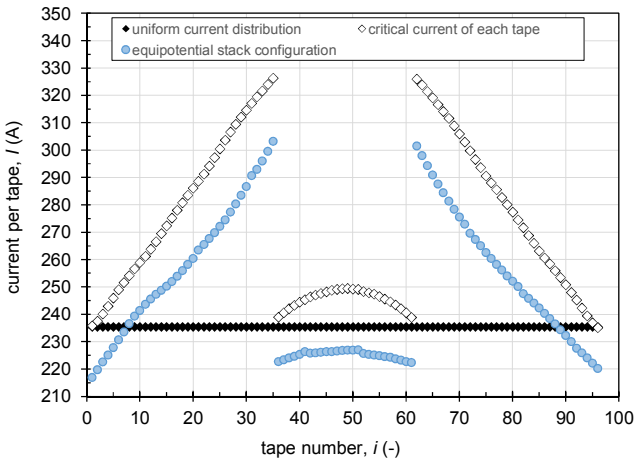

Fig. 6. In case 1 (black and white diamonds), a uniform current distribution to all 96 tapes is assumed for the simulation. In case 2 (blue circles), an equipotential configuration of the 96er stack is assumed. Thus, current can distribute to the different tapes.

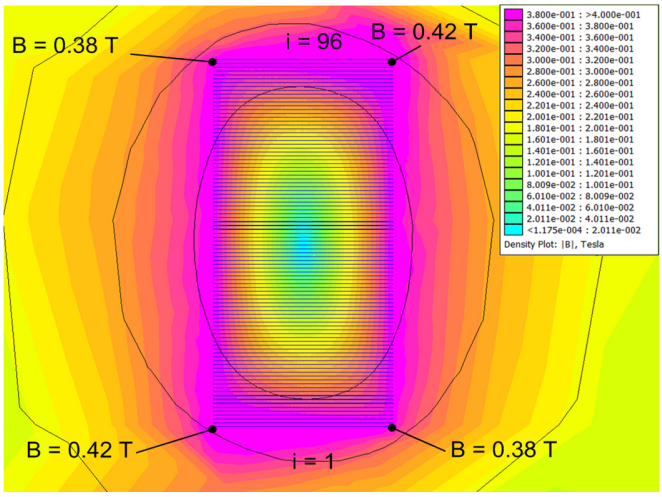

Fig. 7. Magnetic field of the HTS stack. A uniform current distribution to all 96 tapes is assumed. The magnetic field is slightly asymmetric.

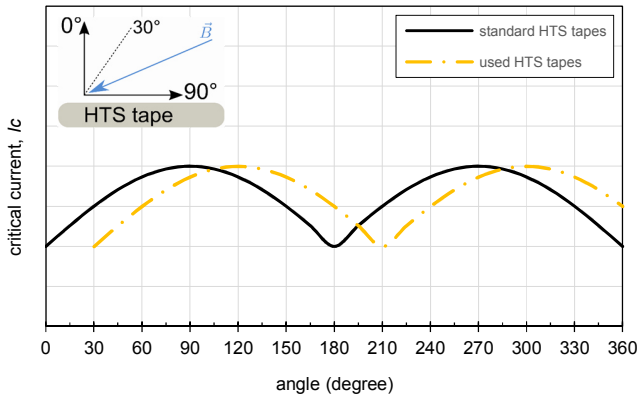

Fig. 8. Schematic critical current dependency on angle of the magnetic field vector for standard tapes (without advanced pinning) and for the tapes used in our current lead.

V. Conclusion

Our aim was to design an efficient and also economic current lead for an operating current of 20 kA. Therefore, we followed the approach to build a three stage cooled current lead, consisting of market proven components. A key element of the current lead is the joint between copper lamellas and HTS tapes, which is realized by a novel soldering process. It has been shown that this soldering process gets acceptable losses of approximately 25 mW per contact.

After the successful assembly of the prototype, first experimental tests to validate our design will follow soon.

Acknowledgment

The author would like to thank the company Vision Electric Super Conductors Ltd., for enabling the development and manufacturing of the current lead. The author also would like to thank the students which contributed to this project.

IEEE/CSC & ESAS SUPERCONDUCTIVITY NEWS FORUM (global edition), January 2017 (Preview 2).
This ASC 2016 manuscript 3LPo2D-04 was submitted to *IEEE Trans. Appl. Supercond.* for possible publication.
DOI: 10.1109/TASC.2017.2655108

REFERENCES

[1] A. Morandi, "HTS dc transmission and distribution: concepts, applications and benefits," *Supercond. Sci. Technol.*, vol. 28, no. 12, 2015, p. 123001.
[2] M. Runde, "Application of High-Tc Superconductors in Aluminum Electrolysis Plants," *IEEE Trans. Appl. Supercond.*, vol. 5, no. 2, 1995, pp. 813–816.
[3] D. Zhang *et al.*, "Testing Results for the Cable Core of a 360 m/10 kA HTS DC Power Cable Used in the Electrolytic Aluminum Industry," *IEEE Trans. Appl. Supercond.*, vol. 23, no. 3, 2013, p. 5400504.
[4] S. Dai *et al.*, "Testing and Demonstration of a 10-kA HTS DC Power Cable," *IEEE Trans. Appl. Supercond.*, vol. 24, no. 2, 2014, pp. 99–102.
[5] R. McFee, "Optimum Input Leads for Cryogenic Apparatus," *Rev. Scientific Instr.*, vol. 30, no. 2, 1959, pp. 98–102.
[6] M. N. Wilson, "Superconducting Magnets," Clarendon Press, 1983.
[7] A. Ballarino, "Large-capacity current leads," *Physica C: Superconductivity*, vol. 468, 2008, pp. 2143–2148.
[8] R. Heller *et al.*, "70 kA High Temperature Superconductor Current Lead Operation at 80 K," *IEEE Trans. Appl. Supercond.*, vol. 16, no. 2, 2006, pp. 823–826.
[9] E. Rizzo, "Simulations for the optimization of High Temperature Superconductor current leads for nuclear fusion applications," Ph.D. dissertation, KIT Scientific Publishing, 2014.
[10] S. Yamaguchi *et al.*, "Refrigeration Process to Realize a Multistage and Gas-Cooled Current Lead," *IEEE Trans. Appl. Supercond.*, vol. 23, no. 3, 2013, p. 4802304.
[11] S. Yamaguchi *et al.*, "A Proposal of Multi-stage current lead for reduction of heat leak," *Physics Procedia*, vol. 27, 2012, pp. 448–451.
[12] L. Bromberg, P. C. Michael, J. V. Minervini, and C. Miles, "Current lead optimization for cryogenic operation at intermediate temperatures," *AIP Conf. Proc.*, vol. 1218, no. 1, 2010, pp. 577–584.
[13] P. C. Michael, L. Bromberg, A. J. Dietz, K. J. Cragin, and C. Gold, "Design and Test of a Prototype 20 kA HTS DC Power Transmission Cable," *IEEE Trans. Appl. Supercond.*, vol. 25, no. 3, 2015, pp. 1–5.
[14] D. Goloubev, "Kühlung eines resistiven HTSL-Kurzschlussstrombegrenzers mit einer Gemisch-Joule-Thomson-Kältemaschine," Ph.D. dissertation, Dresden, 2003.
[15] R. Agsten, "Thermodynamic optimization of current leads into low temperature regions," *Cryogenics*, vol. 13, no. 3, 1973, pp. 141–146.
[16] V. M. R. Zermeño, S. Quaiyum, and F. Grilli, "Open-Source Codes for Computing the Critical Current of Superconducting Devices," *IEEE Trans. Appl. Supercond.*, vol. 26, no. 3, 2016, pp. 1–7.
[17] F. Grilli, F. Sirois, V. M. R. Zermeño, and M. Vojenčiak, "Self-Consistent Modeling of the Ic of HTS Devices: How Accurate do Models Really Need to Be?," *IEEE Trans. Appl. Supercond.*, vol. 24, no. 6, 2014, pp. 1–8.
[18] M. Lao, J. Bernardi, M. Bauer, and M. Eisterer, "Critical current anisotropy of GdBCO tapes grown on ISD–MgO buffered substrate," *Supercond. Sci. Technol.*, vol. 28, no. 12, 2015, p. 124002.